Beam energy dependence of light nuclei (d, t) productions in Au+Au collisions at RHIC

Ning Yu for the STAR Collaboration

Xinyang Normal University
Central China Normal University

Outline

- ✫ Introduction
- ✫ The STAR Experiment
- ✫ Results
- ✫ Summary and Outlook

QCD Phase Diagram

LHC,RHIC

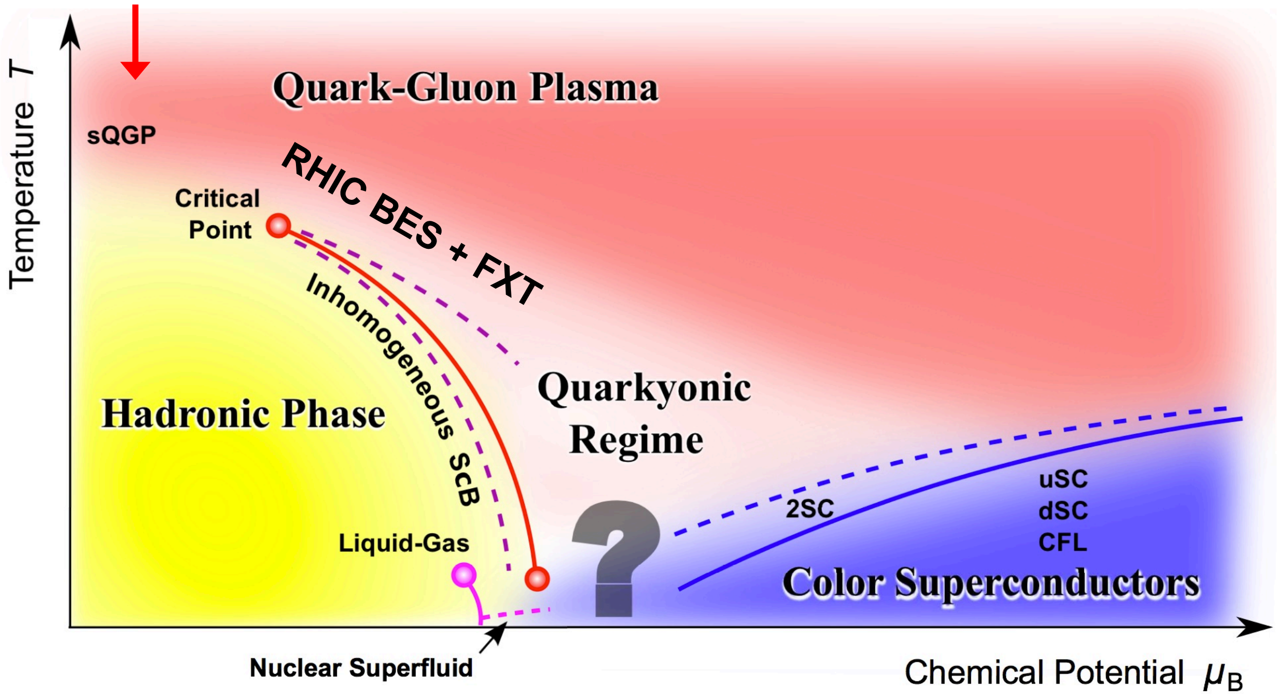

K. Fukushima and C. Sasaki
Prog. Part. Nucl. Phys, 72, (2013) 99

- ✮ High temperature: QGP properties
- ✮ High baryon density:
  - ✓ Critical Point and Phase boundary
  - ✓ Possible New Phase structure : Quarkyonic Matter

fluctuations

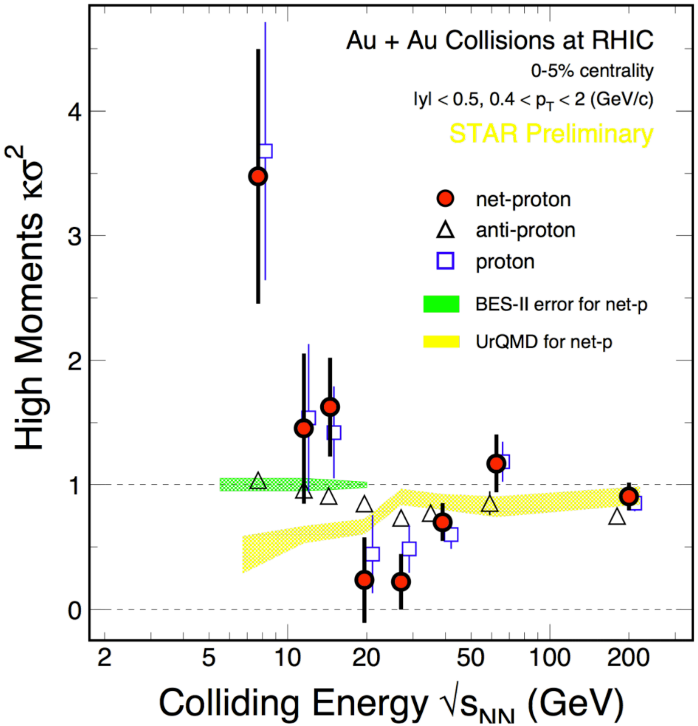

X.F.Luo, N.Xu,
Nucl. Sci. and Tech., 2017,28,112

π -π femtoscopic correlations

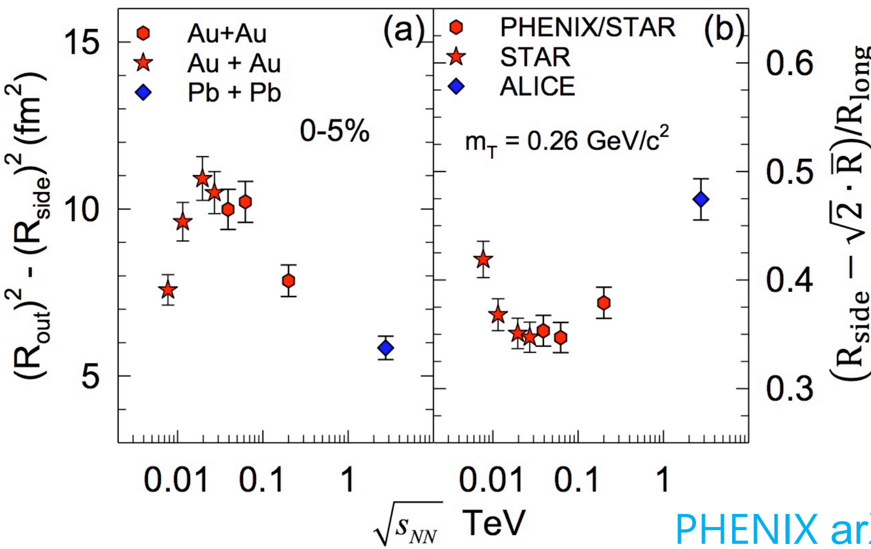

PHENIX arXiv:1410.2559

Phase Transition

Correlations of nucleons
(volume, density)

Light nuclei
(2,3… nucleons)

Light Nuclei Formation in HI Collisions

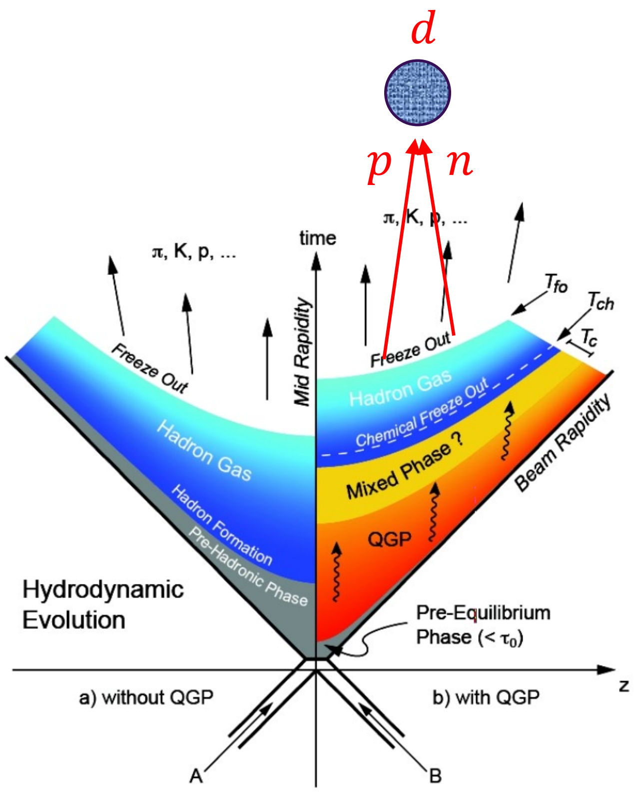

- Coalescence Model : small binding energy (ε), such as d and $\bar{d}$ with binding energy $\varepsilon = 2.2$ MeV, formed via final-state coalescence

$$E_A \frac{d^3 N_A}{dp_A^3} = B_A \left(E_p \frac{d^3 N_p}{dp_p^3} \right)^Z \left(E_n \frac{d^3 N_n}{dp_n^3} \right)^{A-Z} \approx B_A \left(E_p \frac{d^3 N_p}{dp_p^3} \right)^A, \ p_A = A p_p$$

$$B_A \propto V_f^{1-A}$$

Light nuclei produced at the chemical freeze-out might break up and reform between the chemical freeze-out and the kinetic freeze-out.

László P. Csernai, Joseph I. Kapusta Phys. Reps, 131,223(1986)
B. Monreal, *et. al.* PRC60,031901(1999), PRC60,051902(1999)

Light Nuclei Formation in HI Collisions

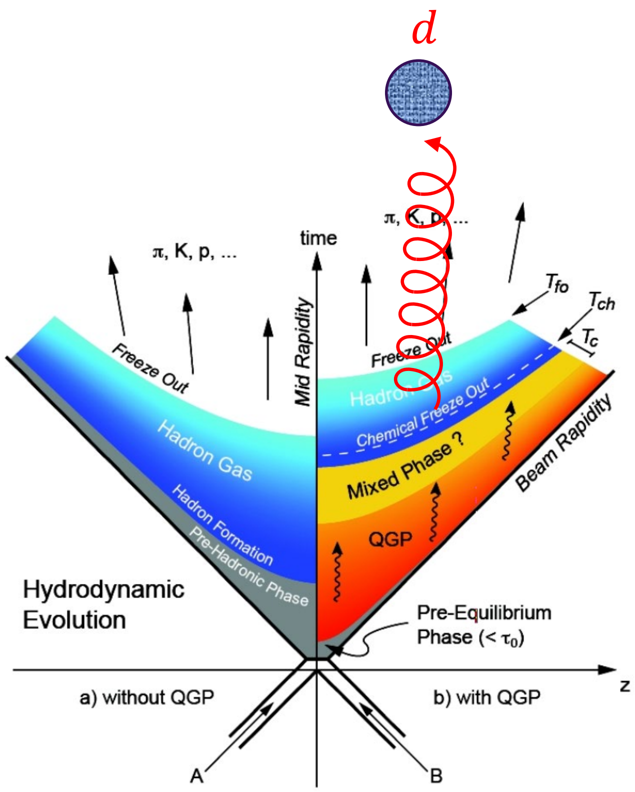

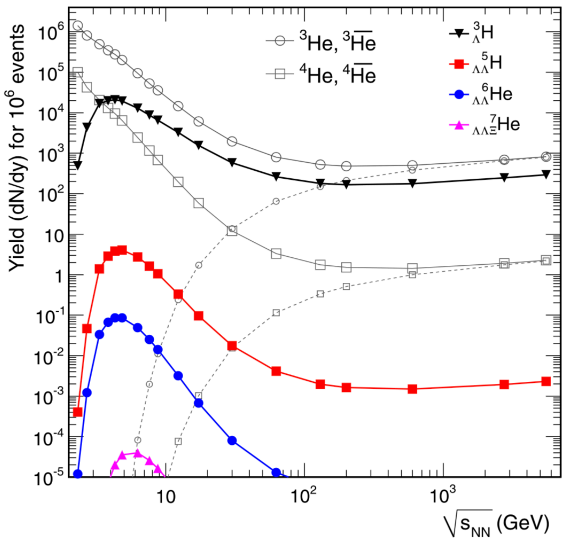

- Thermal Model : emitted at chemical equilibrium, yield fixed at chemical freeze-out for all hadrons

$$N_i = \frac{g_i V}{2\pi^2} m_i^2 T_{ch} K_2\left(\frac{m_i}{T_{ch}}\right) e^{\mu_i/T_{ch}}$$

A. Andronic, P. Braun-Munzinger, J. Stachel and H. Stoecker, PLB697, 203 (2011),

Light Nuclei Formation in HI Collisions

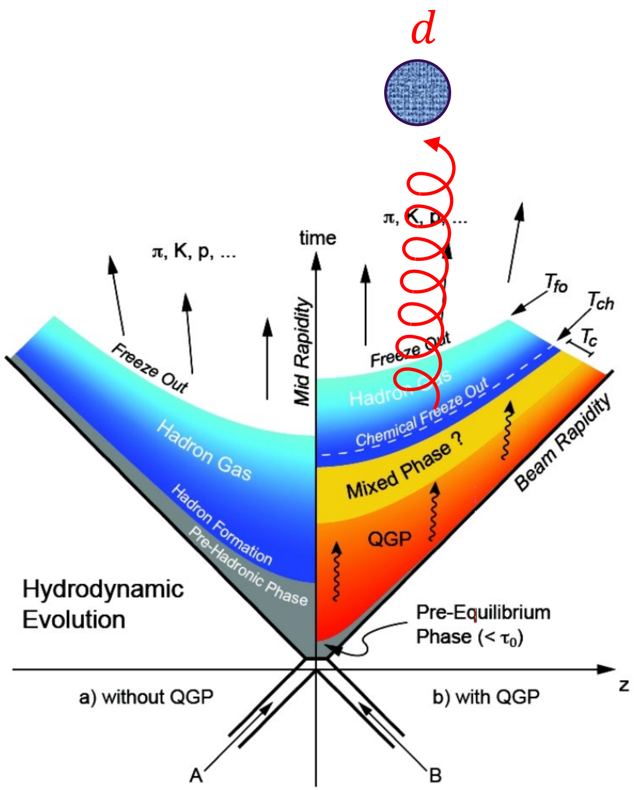

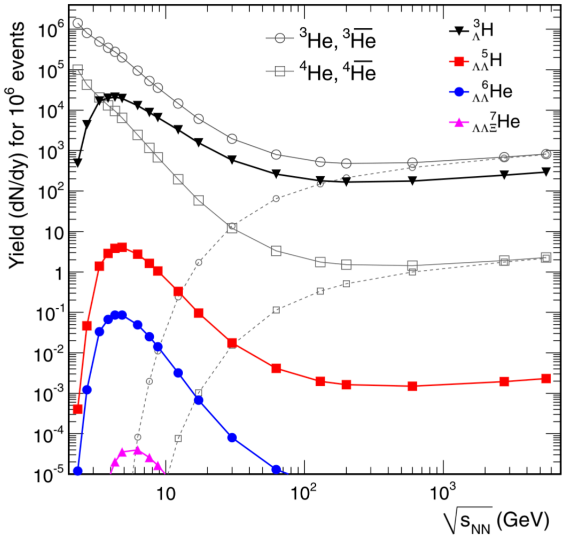

- Thermal Model : emitted at chemical equilibrium, yield fixed at chemical freeze-out for all hadrons

$$N_i = \frac{g_i V}{2\pi^2} m_i^2 T_{ch} K_2\left(\frac{m_i}{T_{ch}}\right) e^{\mu_i/T_{ch}}$$

A. Andronic, P. Braun-Munzinger, J. Stachel and H. Stoecker, PLB697, 203 (2011),

Light nuclei may serve as probes of space-momentum density and correlation of nucleons at freeze-out.

RHIC Beam Energy Scan

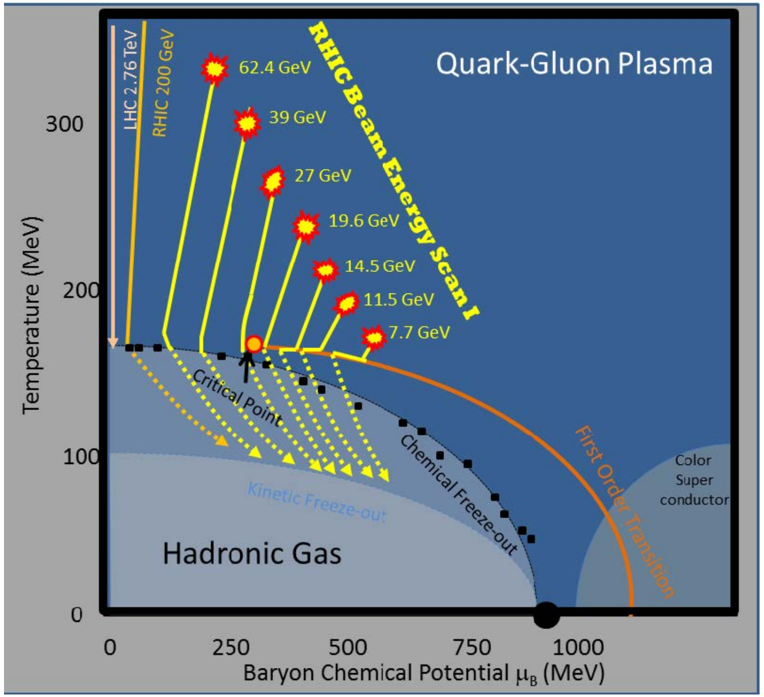

- ✯ BES-I Au+Au collisions at $\sqrt{s_{NN}} = 7.7$, 11.5, 14.5, 19.6, 27, 39 and 62.4 GeV
  - ✓ Search for conjectured QCD critical point
  - ✓ Search for the first-order phase transition
  - ✓ Search for the onset of key QGP signatures

STAR :arxiv 1007.2613

$\sqrt{s_{NN}}$(GeV)	7.7	11.5	14.5	19.6	27	39	62.4	200
N_{eve}(M)	4	11	27	40	71	133	67	480
μ_B(MeV)	420	315	260	205	155	115	72	20

J. Cleymans, H. Oeschler, K. Redlich, and S. Wheaton PRC 73,034905 (2006)

The Solenoidal Tracker At RHIC

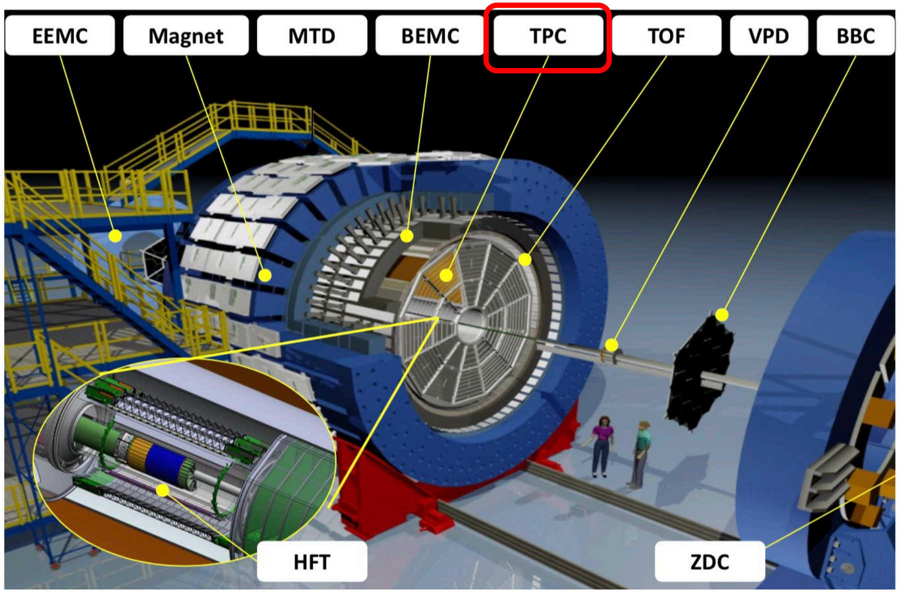

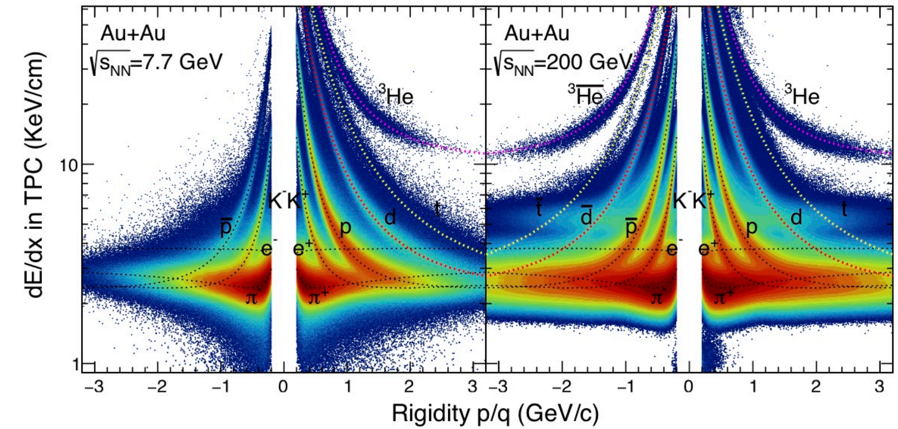

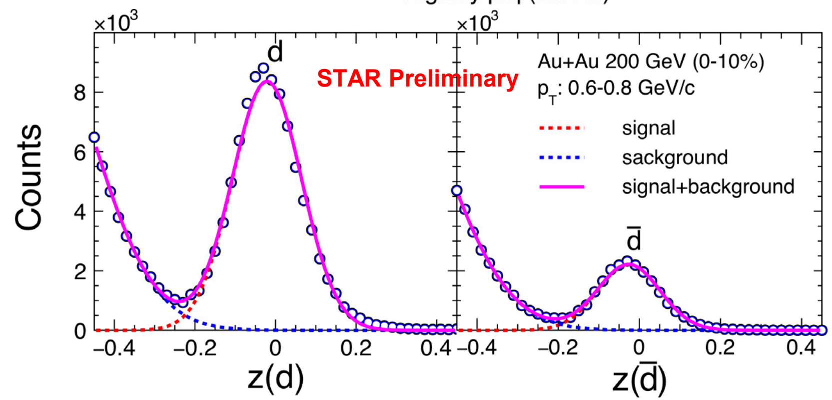

Time Projection Chamber（TPC）

- ☆ Charged Particle Tracking
- ☆ Momentum reconstruction
- ☆ Particle identification by ionization energy loss (dE/dx)
- ☆ Pseudorapidity coverage |η| < 1.0

$$z_d = \log\left(\frac{\langle dE/dx\rangle}{\langle dE/dx\rangle_d^{BB}}\right)$$

BB : Bethe-Bloch,H. Bichsel, Nucl. Instrum. Meth. A 562, 154 (2006).

The Solenoidal Tracker At RHIC

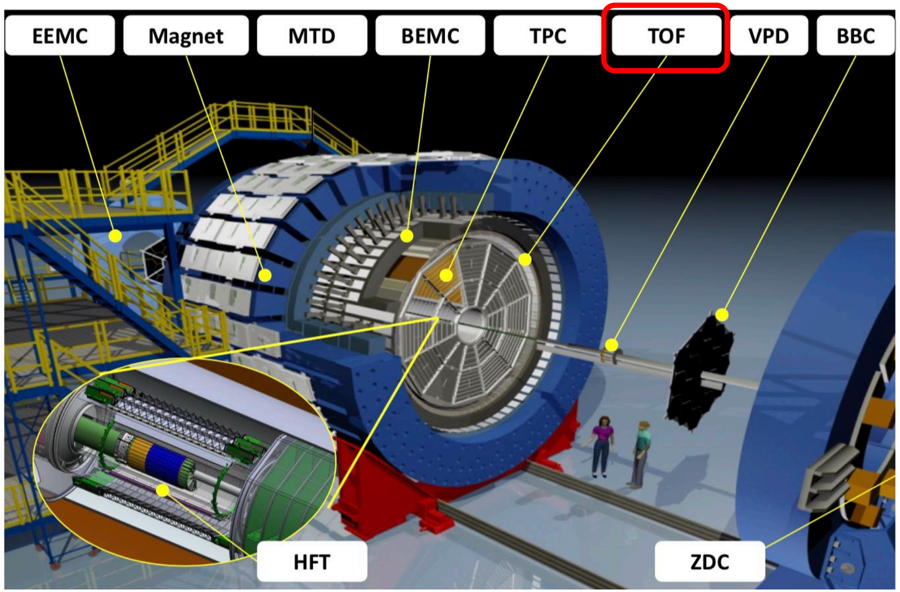

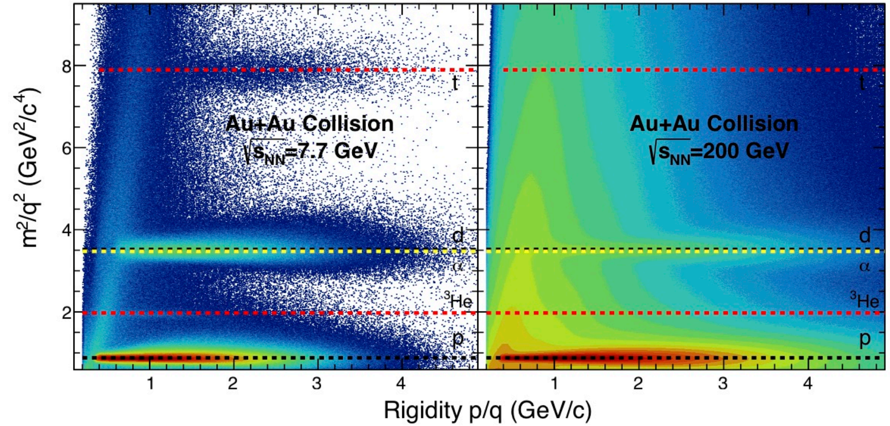

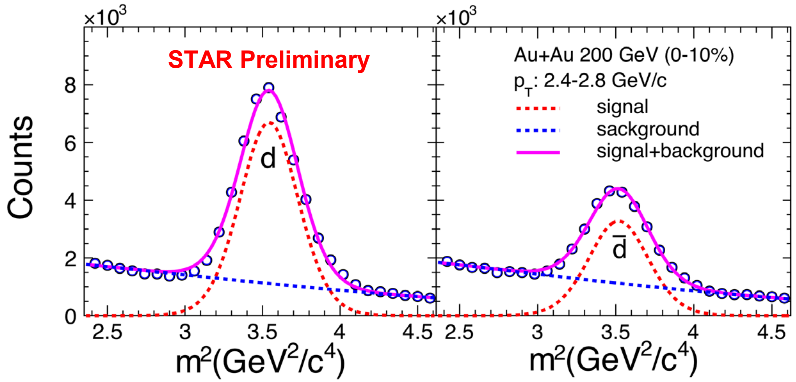

Time Of Flight (TOF)

- ☆ Particle identification m^2
- ☆ Pseudorapidity coverage $|\eta| < 0.9$

$$\left(\frac{m}{q}\right)^2 = \left(\frac{p}{q}\right)^2 \left(\frac{c^2 t^2}{L^2} - 1\right)$$

Transverse Momentum Spectra

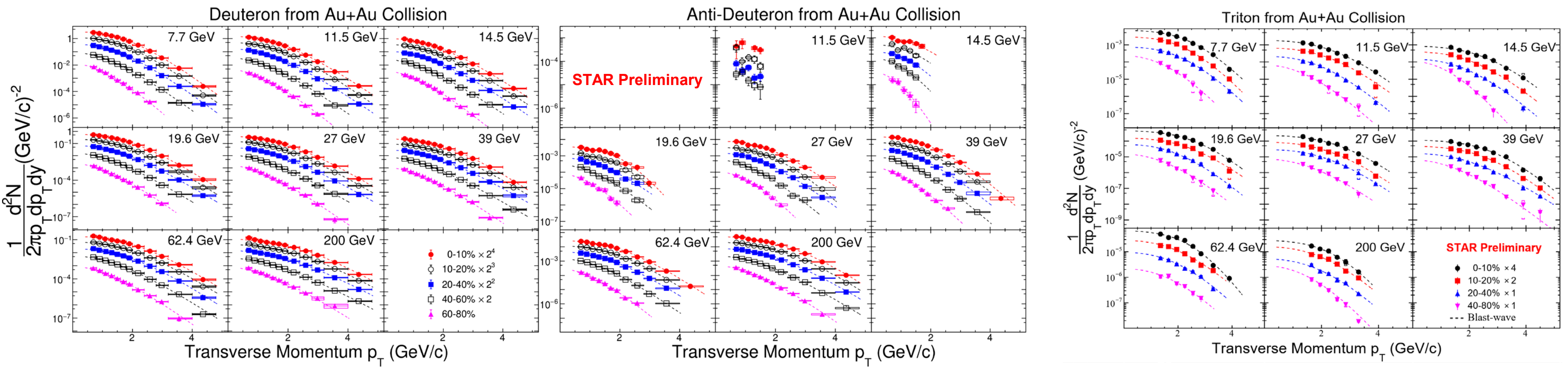

☆ Midrapidity ($|y| \leq 0.3$) transverse momentum distribution of $d(\bar{d})$ from Au+Au Collisions

☆ Midrapidity ($|y| \leq 0.5$) transverse momentum distribution of t from Au+Au Collisions

☆ Dash line: blast-wave function fits

$$\frac{\mathrm{d}^2 N}{p_T dp_T} \propto \int_0^R r\mathrm{d}r m_T I_0\left(\frac{p_T \sinh\rho}{T}\right) K_1\left(\frac{m_T \cosh\rho}{T}\right) \qquad \rho = \tanh^{-1}\left(\beta \frac{r}{R}\right)$$

E. Schnedermann, J. Sollfrank, and U. Heinz, PRC 73,034905 (2006)

Integral Yield dN/dy

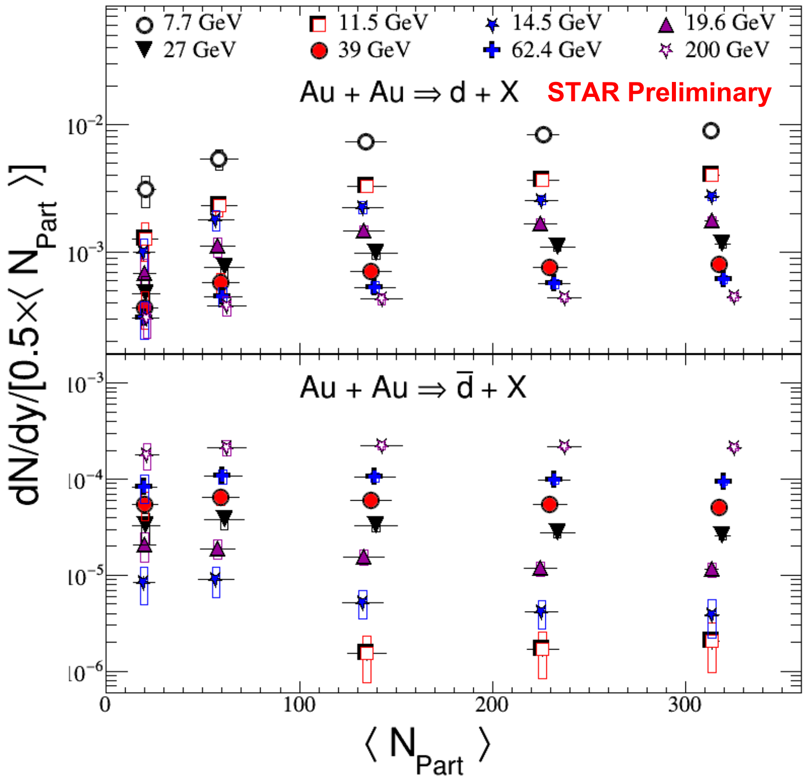

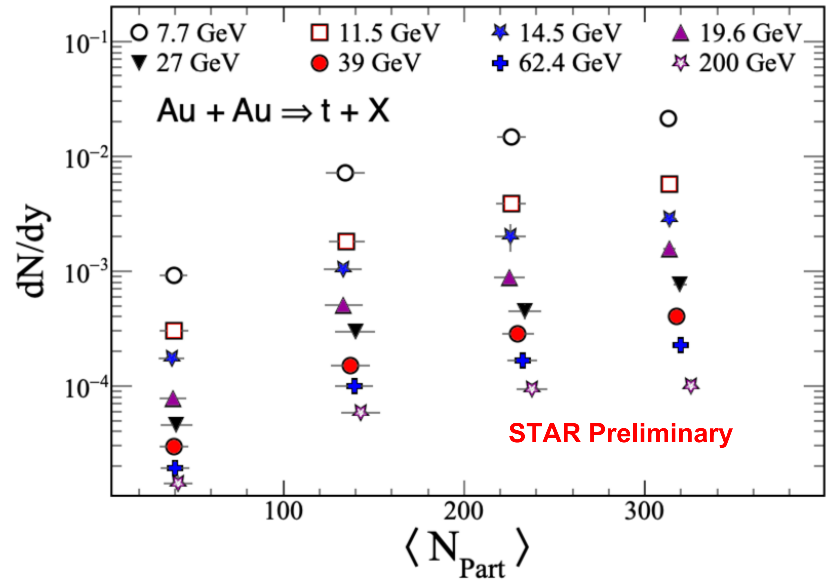

- ☆ dN/dy for d and t is smaller at higher energy: baryon stopping
- ☆ dN/dy for $\bar{d}$ increases with increasing energy: baryon pair production
- ☆ N_{part} scaled dN/dy for $\bar{d}$ show weak centrality dependence, for d increase slightly from peripheral to central collisions

$\langle p_T \rangle$

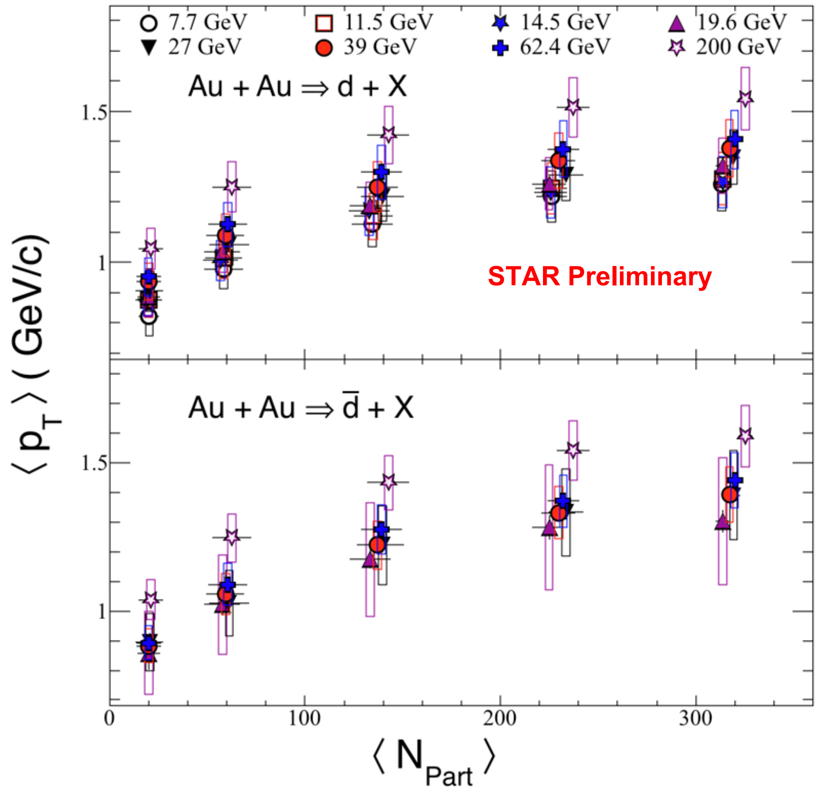

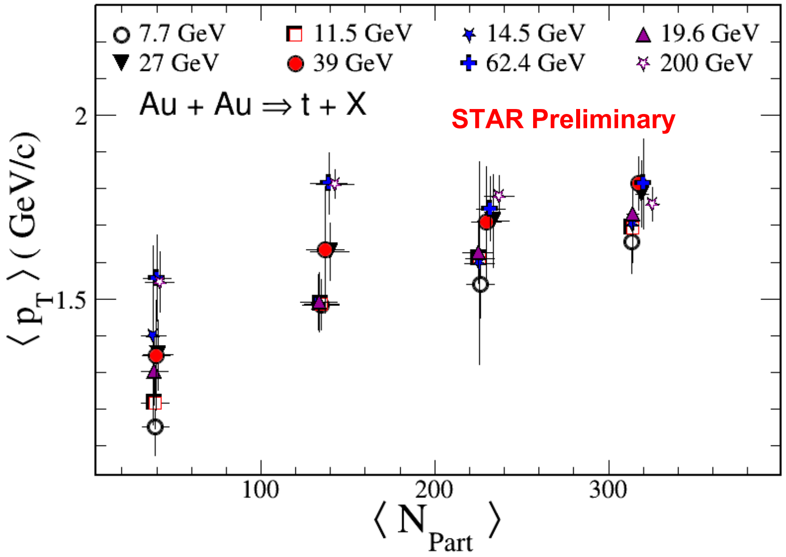

- ☆ $\langle p_T \rangle$ decreases from central to peripheral collisions
- ☆ $\langle p_T \rangle$ of d and $\bar{d}$ are consistent within uncertainties

Particle Ratios

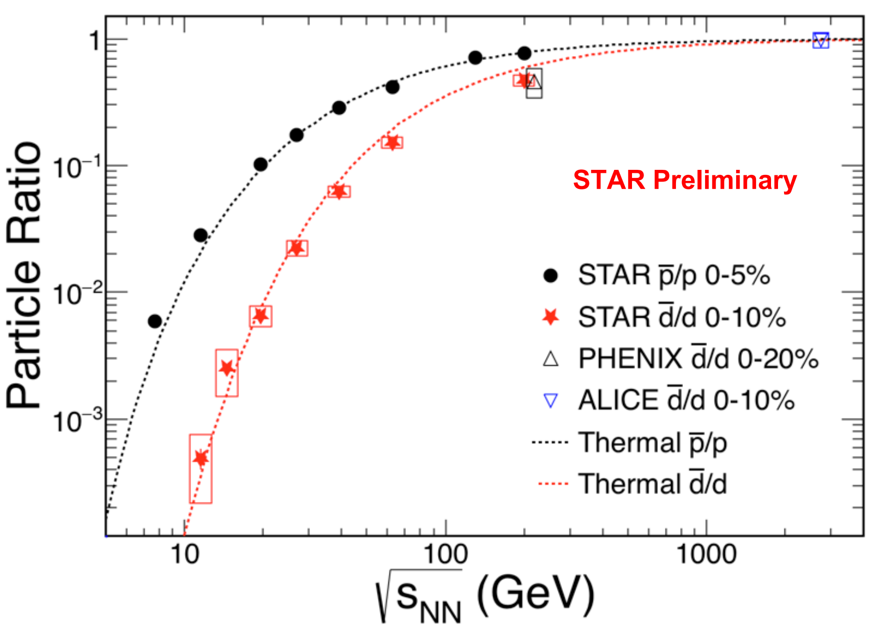

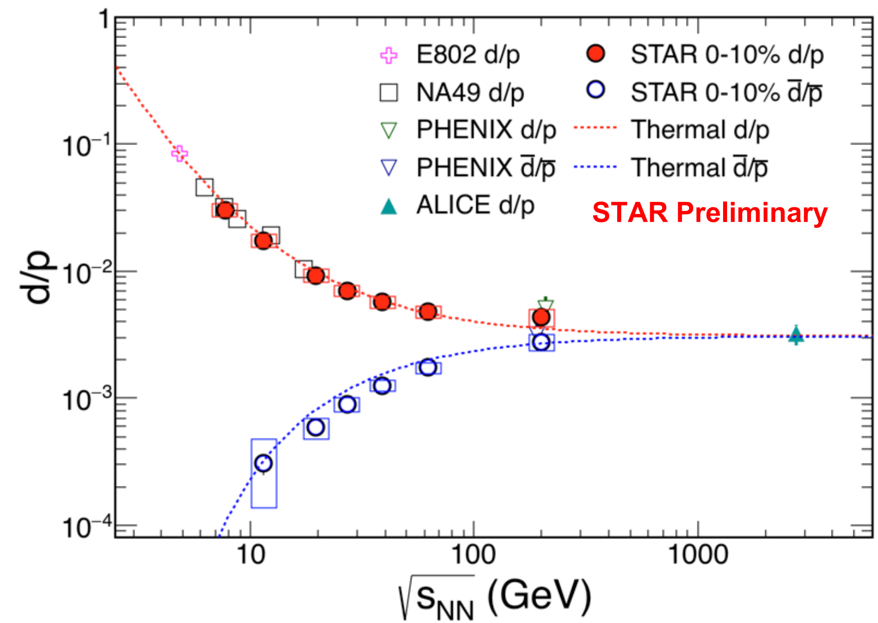

- ☆ $N(\bar{d})/N(d)$ decreases with decreasing energy
- ☆ $N(\bar{d})/N(d)$ ratio decreases as a function of collision centrality
- ☆ Thermal model can describe $N(\bar{p})/N(p)$ and $N(\bar{d})/N(d)$ in a wide energy range.

- ☆ The d/p ratios from thermal model prediction are consistent with the data from SIS up to LHC energies.

The lines are from thermal model prediction
A. Andronic, P. Braun-Munizinger, J. Stachel, H. Stöcker, PLB697 (2011)203

d/p^2 and $\bar{d}/\bar{p}^2$ Ratios

- In thermal model with GCE (grand canonical ensemble), d/p^2 and $\bar{d}/\bar{p}^2$ should be the same if isospin effect can be neglected

$$\frac{\mu_Q}{T} = \frac{1}{2}\ln\left(\frac{\bar{d}/\bar{p}^2}{d/p^2}\right)$$

- The μ_Q/T can also be obtained by

$$\frac{\mu_Q}{T} = \frac{1}{2}\ln\left(\frac{\pi^+}{\pi^-}\right)$$

- The results from π are closer to zero than those from d/p^2.
  - strong-decay contribution to π and p
  - non-thermalization

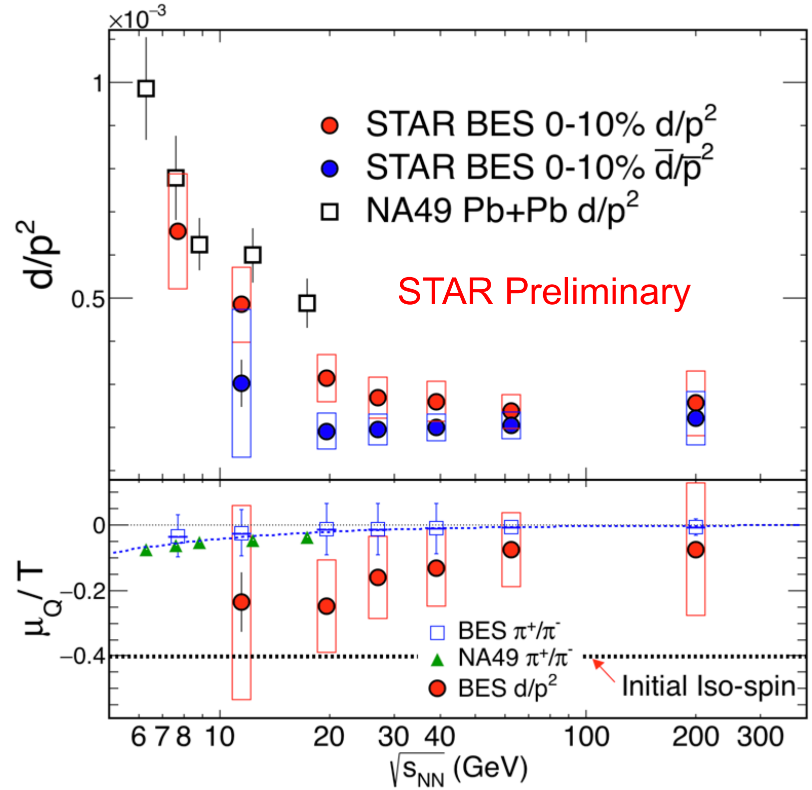

NA49, PRC 94, 044906 (2016)

B_2 v.s. m_T and Collision Centrality

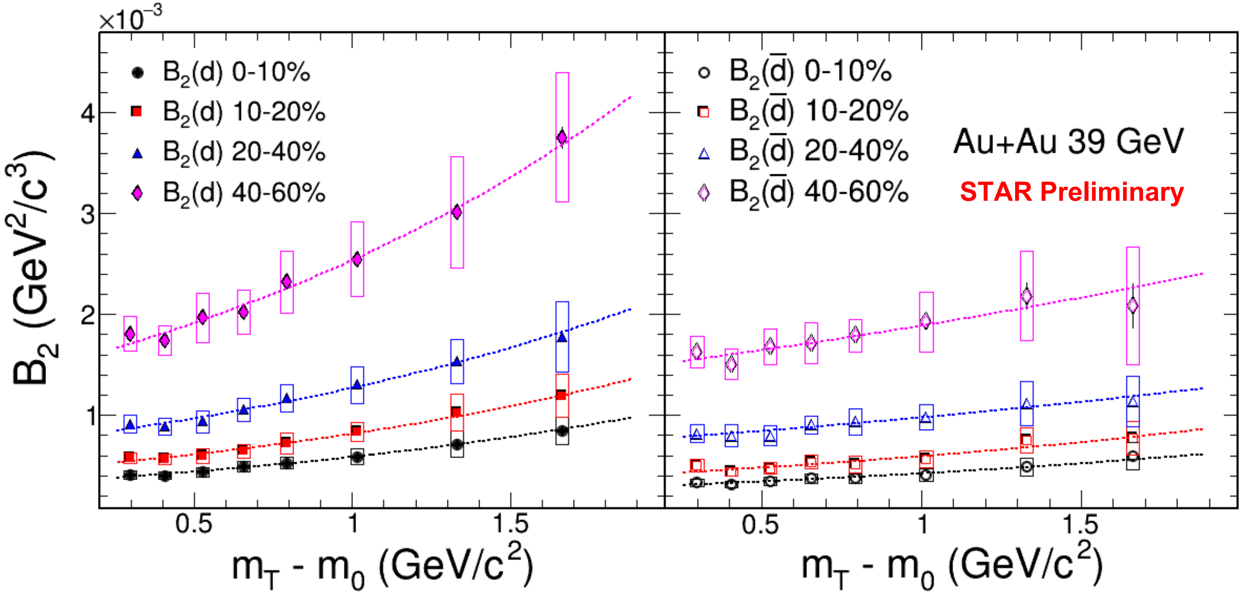

$$B_2 = a \cdot \exp[b(m_T - m)]$$

NA44, EPJ C. 23, 237 (2002)

- ☆ The values of B_2 increase as a function of m_T and decreases with collision centrality : collective expansion
- ☆ $B_2\left(\overline{d}\right)$ are smaller than that of $B_2(d)$, anti−baryon freeze-out at a larger source

Coalescence Parameters vs. Collision Energy

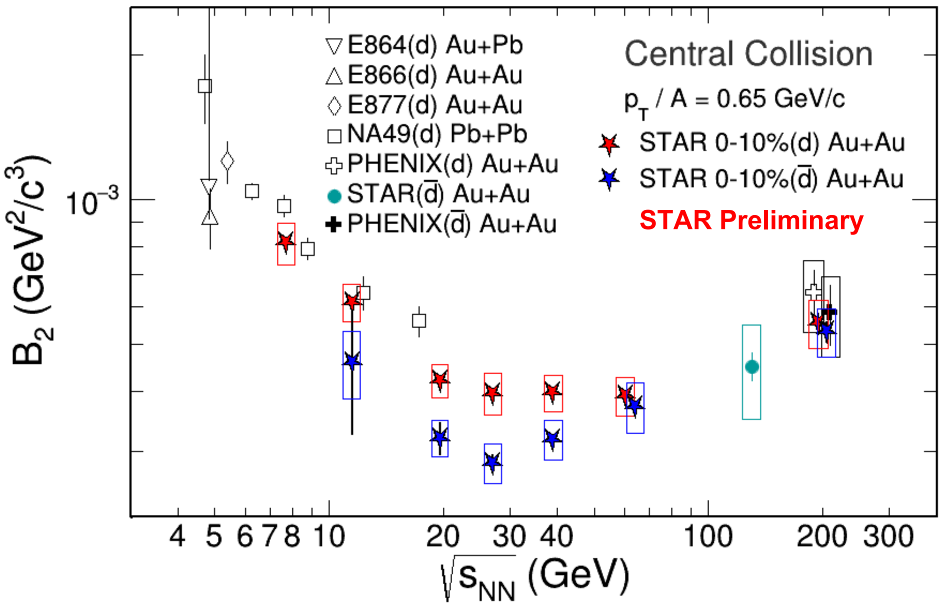

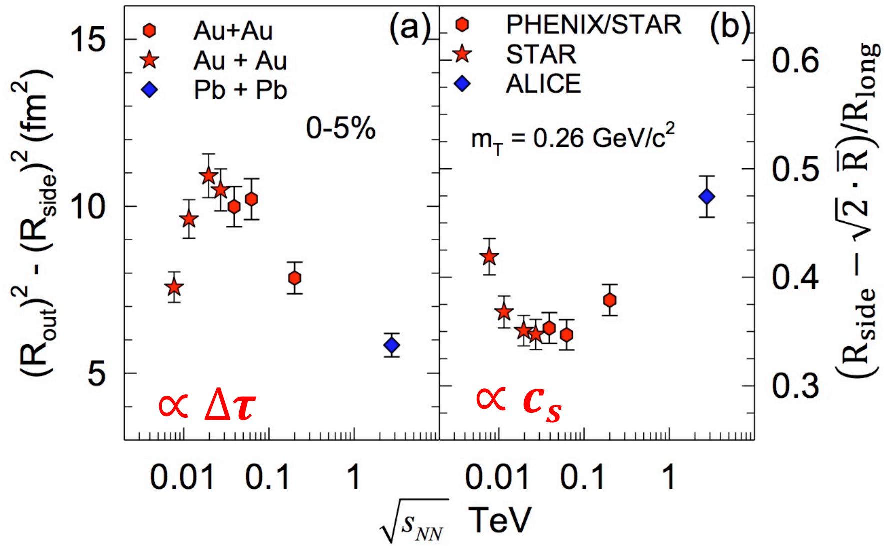

arXiv:1410.2559

☆ B_2 decreases with collision energy. A minimum around $\sqrt{s_{NN}} = 20$ GeV : **change of EOS?!**

☆ $B_2(\bar{d})$ values are systematically lower than that of $B_2(d)$ implying emitted source of anti-baryons is larger than those of baryons.

B_2 and $\sqrt{B_3}$

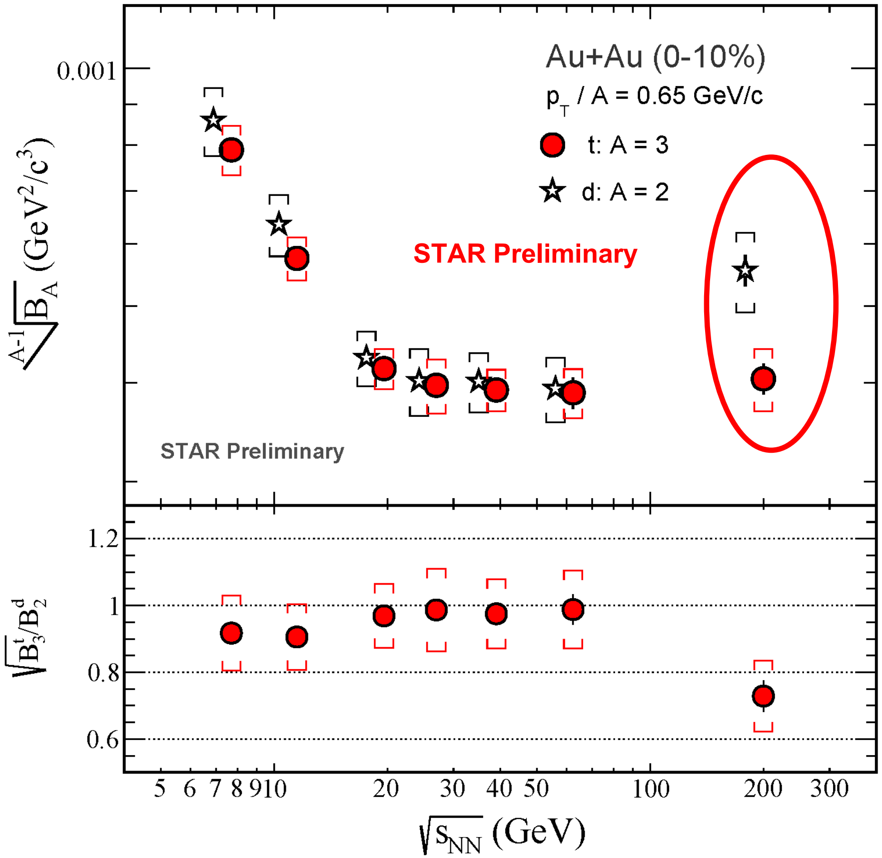

- ☆ B_2 and $\sqrt{B_3}$ are consistent within uncertainties except 200 GeV.
- ☆ Different production mechanism for d and t at 200 GeV ?
- ☆ Competition of thermal production and coalescence production?

Nucleon Relative Density Fluctuation

- ✩ The particle ratios of light nuclei is sensitive to the **nucleon density fluctuation** at kinetic freeze-out.

  (Caution: This conclusion is based on **coalescence model**)

$$\Delta n = \frac{1}{g}\frac{N_t N_p}{N_d^2} - 1$$

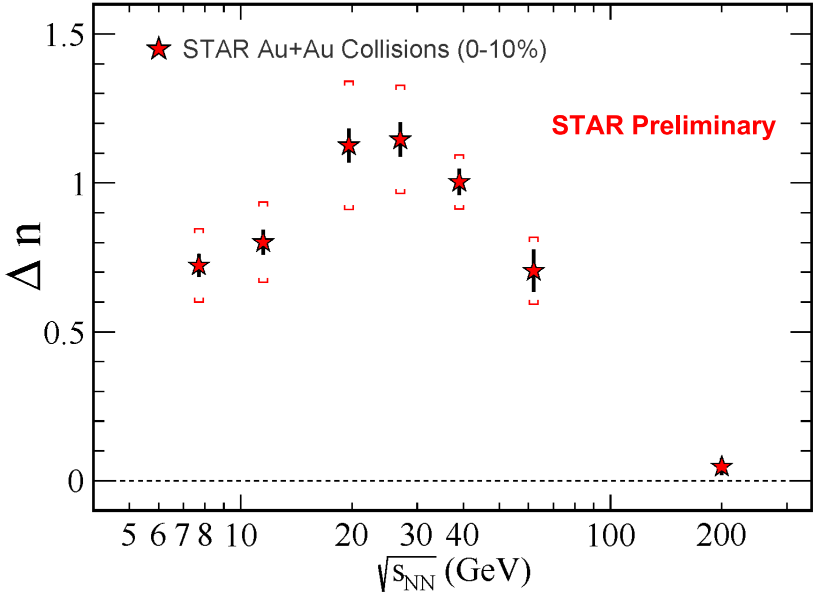

Neutron density fluctuation Δn shows a non-monotonic behavior on collision energy.

Peak around 20 GeV.

Summary

- ✮ STAR systematic results of $d(\bar{d})$ and t production (dN/dy, $\langle p_T \rangle$) from Au + Au collisions at $\sqrt{s_{NN}}$ = 7.7, 11.5, 14.5, 19.6, 27, 39, 62.4 and 200 GeV
- ✮ Coalescence parameter B_2 for d and $\bar{d}$ are extracted. $B_2(d)$ and $B_2(\bar{d})$ are found to be different in the most central collisions for the first time.
- ✮ Similar to the pion HBT and net-proton high moments, around $\sqrt{s_{NN}} = 20$ GeV, B_2 reaches a minimum suggesting the change of EOS around the energy.
- ✮ B_2 and $\sqrt{B_3}$ are consistent within uncertainties except 200 GeV.
- ✮ Neutron density fluctuation Δn shows a non-monotonic behavior on collision energy.